The Chemist
Journal of the American Institute of Chemists

Crosslinked Alginate–Acrylic Acid–PVA Hydrogel for Efficient Trypan Blue Removal: Swelling Behavior, Adsorption Isotherms, and Regeneration Performance

Haider Ali Dhaher[1], Aseel M Aljeboree*[2], Khawla K. Jasim[3]

[1,3]Department of Chemistry, College of Sciences, University of Al-Muthanna, Al-Samawah, Iraq
[2]Department of Chemistry, College of Sciences for Girls, University of Babylon, Hilla, Iraq
**Corresponding author (E-mail: annenayad@gmail.com)*

Abstract: In this study, a cross-linked sodium alginate-graft-poly(acrylic acid-co-polyvinyl alcohol) (SA-g-poly(AAC-co-PVA)) hydrogel was successfully prepared through free-radical polymerization and evaluated for its ability to remove Trypan Blue (TB) dye from aqueous media. The samples were characterized using Fourier Transform Infrared Spectroscopy (FTIR), Thermogravimetric Analysis (TGA), X-ray Diffraction (XRD), Transmission Electron Microscopy (TEM), and Field Emission Scanning Electron Microscopy (FESEM). They confirmed the formation of a porous hydrogel network with a predominantly amorphous structure and adequate thermal stability. The adsorption performance was systematically examined under different operational conditions, including the effect of a 200 mg L^{-1} dye concentration on the adsorption of 0.07g of hydrogel at pH 7 and 30°C. The results showed a clear dependence on solution pH, where acidic environments favored dye uptake due to reduced electrostatic repulsion between the anionic dye molecules and the protonated hydrogel surface. A pronounced decline in both removal efficiency (E%) and adsorption capacity (Qe) was observed with increasing pH solution. At pH 3, the hydrogel exhibited excellent adsorption performance, achieving an E of 96% and a Qe of 480 mg g^{-1}. However, when the pH was increased to 11, these values dropped significantly to 41% and 210 mg g^{-1}, respectively, indicating that acidic conditions strongly favor the adsorption process. Increasing the adsorbent dosage increased overall removal efficiency, although a decrease in adsorption capacity per unit mass was observed. Increasing the hydrogel mass from 0.01 g to 0.10 g increased E% from ~50% to ~97%, whereas Qe decreased from ~1500 mg g^{-1} to ~300 mg g^{-1}. The adsorption process proceeded rapidly, achieving an equilibrium capacity of approximately 350 mg g^{-1} within 25 min and reaching about 410 mg g^{-1} at longer contact times. Analysis of equilibrium data revealed that the Freundlich isotherm model provided a better fit (R^2 = 0.9883), indicating multilayer adsorption on heterogeneous sites within the grafted polymer network. Regeneration experiments demonstrated that the hydrogel retained nearly 60% of its initial removal efficiency after five consecutive adsorption–desorption cycles, highlighting its potential for

repeated use. Overall, the prepared hydrogel shows promise as an effective, reusable adsorbent for removing Trypan Blue from wastewater.

Key Words: Polymer composite**,** trypan blue dye**,** adsorption**,** wastewater treatment**,** regeneration

1. Introduction

Water contaminated with dyes requires treatment to remove them using various adsorbents or techniques prior to discharge into local drainage systems or natural water bodies. Dyes are employed across numerous industries, including textiles, cosmetics, ink, plastics, paper, food, pharmaceuticals, pulp, leather, printing, paints, and rubber, owing to their high solubility in water and capacity to impart intense color [1-3]. Trypan blue (TB) is a water-soluble azo dye, classified as an anionic acidic dye, with a molar mass of 960.81 g/mol and a chemical formula of ($C_{34}H_{24}N_6Na_4O_{14}S_4$). It is used in biological staining, vitreoretinal surgery, cell viability assessment, and food coloring processes. However, Trypan Blue (TB) is cytotoxic to cells. Empirical studies have demonstrated that exposure of human retinal pigment epithelial cells (ARPE-19) to TB *in vitro* induces cellular toxicity and reduced viability, with the severity of these effects contingent on the dye concentration and exposure duration. Furthermore, elevated TB concentrations pose a threat to aquatic organisms and the environment. The discharge of untreated water contaminated with this dye can adversely affect natural water bodies, disrupt aquatic ecosystems, and pose significant risks to human and environmental health [4-6].

The release of untreated water contaminated with this dye can adversely affect natural water resources, disrupt aquatic ecosystems, and pose significant health risks to humans, including toxicity and carcinogenicity. To protect the environment from contamination, it is imperative to eliminate TB discharges from various industries in water sources. The issue of dye pollution in water has led to the development of numerous water treatment methods, including advanced oxidation processes, ion exchange, deep eutectic solvents, coagulation-flocculation, adsorption, electrocoagulation, wet oxidation, sedimentation, arc discharge, membrane bioreactors, phytoremediation, reverse osmosis, sequencing batch reactors, and membrane filtration. Among these, adsorption is recognized as one of the most commonly employed treatment techniques because of its cost-effectiveness, simplicity, high efficiency, and environmental compatibility. Various adsorbents, such as clay, hydrogels, activated carbon, and graphene oxide, have been utilized [7,8].

Hydrogels, also known as superabsorbent polymers, are considered innovative materials due to their versatility and Biocompatibility. They consist of three-dimensional cross-linked polymer networks that are water-soluble but swell upon contact with water, enabling them to absorb water and biological fluids without compromising their structural integrity. This absorption capability is attributed to the presence of hydrophilic groups, such as (–OH, – CONH, $–CONH_2$, –COOH, and $-SO_3H$) in the polymer chain [9,10]. These hydrogels can absorb additional biological fluids, and their expanded state allows them to retain substantial amounts of fluid. They have garnered significant attention for their

applications in biomedical, environmental, energy, and engineering fields due to their enhanced water absorption and Biocompatibility. Despite the development of various types of hydrogels, there remains a need for non-toxic, eco-friendly hydrogels that can be easily prepared with the desired properties [11-13].

Many inorganic clay minerals, such as kaolin, bentonite, and attapulgite, along with natural polymeric materials, including polysaccharides (sodium alginate, starch, cellulose, and chitosan), have been employed to develop eco-friendly organic–inorganic superabsorbent composites to reduce production costs and enhance performance. Sodium alginate (SA), an anionic polysaccharide derived from brown seaweed, has been extensively investigated because of its non-toxic nature, biodegradability, and ability to form gels in the presence of divalent cations such as Ca^{2+}. SA is renowned for its exceptional film-forming and gelation properties, rendering it widely utilized in biomedicine, food packaging, and environmental remediation [14,15].

Acrylic acid (AA), a synthetic monomer bearing a carboxylic acid group, is commonly used in hydrogel production due to its ability to impart significant hydrophilicity to the gel. When copolymerized with natural polymers, such as sodium alginate, it enhances mechanical strength and water-absorption capacity while improving the hydrogel's surface characteristics [16,17]. The resulting hybrid or composite hydrogels integrate the advantages of both natural and synthetic materials, making them popular for applications such as drug delivery, wound dressing, biosensing, agriculture, and wastewater treatment. Recently, SA/AA hydrogels have demonstrated considerable potential as effective adsorbents for removing organic dyes and heavy metals from contaminated water, particularly when modified with nanoparticles or other functional fillers to enhance their adsorption capacity and durability [18]. This study aims to develop and evaluate a SA/AA hydrogel for the efficient adsorption and regeneration-based removal of trypan blue dye from aqueous solutions. The research focuses on the hydrogel's structural properties and its performance across multiple cycles.

2. Experimental Part

Materials

Sodium alginate (SA, purity 99%) was used as the main biopolymer backbone, and acrylic acid (AA, purity 98%) was employed as the grafting monomer. Poly(vinyl alcohol) (PVA, ≥99% purity) was used as a hydrophilic polymer to enhance the mechanical stability of the hydrogel network. Potassium per sulfate (KPS, purity 97%) was used as a free-radical initiator, and N, N′-methylene bisacrylamide (MBA, purity 99%) was used as a cross-linking agent. Trypan Blue (TB) dye was selected as the model anionic dye for the adsorption experiments. Hydrochloric acid (HCl) and sodium hydroxide (NaOH) solutions were used to adjust the pH of the samples. All chemicals were of analytical grade, purchased from Sigma-Aldrich, and used as received without further purification. Deionized water was used in all experiments.

Preparation of SA-g-poly(AAC-co-PVA) Hydrogel

The hydrogel was synthesized via free-radical polymerization using sodium alginate (SA), acrylic acid (AA), and poly(vinyl alcohol) (PVA) as monomeric components. Initially, a 2 wt% SA solution was prepared by dissolving 0.50 g of sodium alginate in 20 mL of deionized water under magnetic stirring at 60°C until complete homogenization. In parallel, 0.50 g of PVA was dissolved in 30 mL of deionized water at 80°C to obtain a clear polymer solution, which was subsequently cooled to room temperature. The PVA solution was then combined with the SA solution to form a blended biopolymeric matrix. Separately, the monomer mixture was prepared by diluting 10 mL of acrylic acid (AA; 0.14 mol) with 3 mL of deionized water, followed by the addition of potassium persulfate (KPS; 0.05 g, 0.18 mmol) as the radical initiator and N,N′-methylene bisacrylamide (MBA; 0.05 g, 0.32 mmol) as the covalent cross-linker. This mixture was stirred for 30 min to ensure uniformity. The SA/PVA blend was gradually added to the AA/KPS/MBA solution under continuous stirring to ensure complete dispersion of all components. The final precursor mixture was cast into Petri dishes and thermally polymerized at 60°C for 1–2 h, forming a cross-linked three-dimenional hydrogel network. After gelation, the hydrogels were removed, repeatedly washed with deionized water to remove unreacted species, and dried at 50–60°C to constant mass. This preparation method yielded a mechanically stable hydrogel with enhanced structural integrity and high-water absorption capacity, owing to the combined roles of SA, PVA, and the covalently cross-linked AA network.

Swelling Ratio

Water adsorption studies are critical for evaluating the performance of hydrogel-based adsorbents, as their swelling behavior directly reflects their porosity, hydrophilicity, and accessibility of active sites. These studies quantify the material's ability to uptake and retain water under controlled environmental conditions, such as fixed temperature, humidity, and immersion time.

The swelling behavior is commonly expressed as the swelling ratio (SR), which represents the percentage increase in mass of the hydrogel due to water uptake. This parameter provides a reliable measure of the hydrogel's water-holding capacity and structural flexibility and is calculated using the following equation (1) [19]:

$$(\mathrm{SR}\ \%) = \frac{w_s - w_d}{w_d} \times 100 \quad (1)$$

where w_s is the weight of the swollen hydrogel (g), and Wd is the weight of the dry hydrogel (g).

Study Gel Content

The gel content (Gc%) of the (SA-g-poly(AAC-co-PVA)) hydrogel was determined to quantify the fraction of the hydrogel network that remains insoluble in water. Initially, the hydrogel samples were dried and weighed, then immersed in distilled water for 24 h at 25°C to extract the soluble components. After extraction, the samples were dried again and reweighed. The gel content (Gc%) was calculated using equation 2:

$$(\text{Gc}\%) = \frac{\text{Md}}{\text{Mo}} \times 100 \quad (2)$$

where Md represents the weight of the dried sample after extraction, and Mo corresponds to the initial weight of the dried sample before extraction.

Preparation of Trypan Blue Dye Solution

Figure 1 shows the chemical structure of Trypan Blue dye is an anionic azo dye with the molecular formula ($C_{34}H_{24}N_6Na_4O_{14}S_4$) and a molecular weight of 960.81 g.mol^{-1} illustrates the chemical structure of the TB dye.

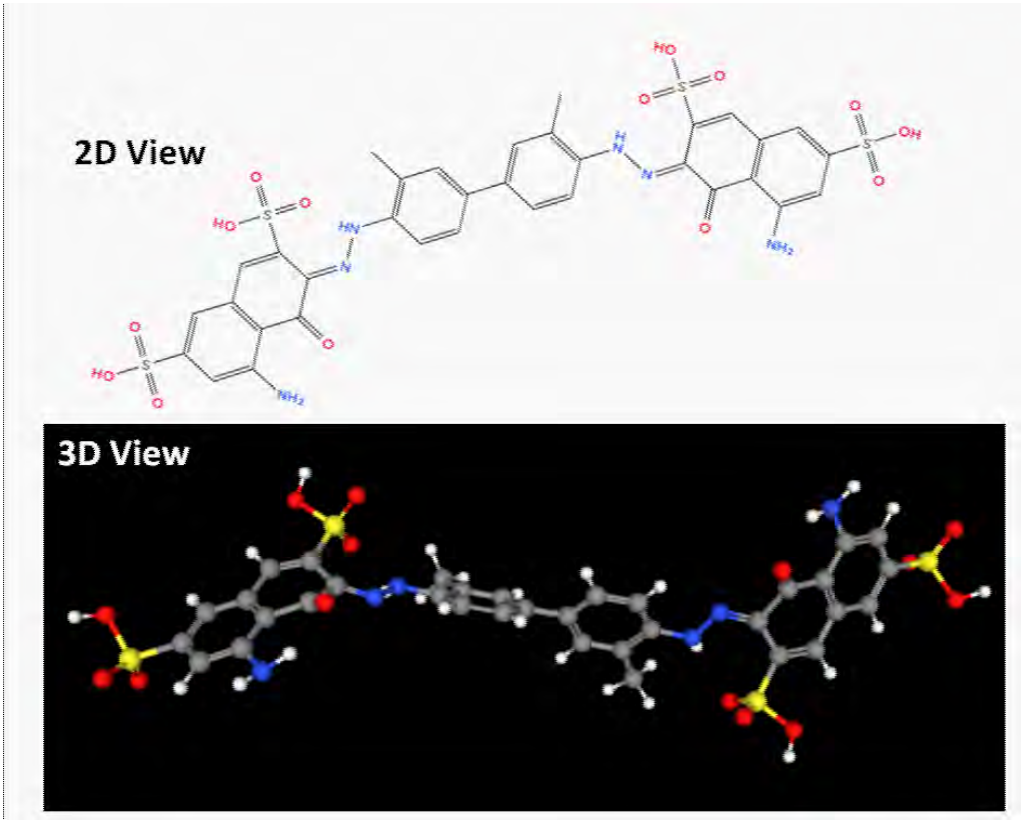

Fig 1. Chemical Structure of Trypan Blue (TB)

A stock solution at 1000 mg L^{-1} was prepared by dissolving 0.1 g of dye powder in 100 mL of distilled water. The maximum absorption wavelength (λ_{max}) was determined using a

UV-Vis spectrophotometer, and the maximum absorbance peak was observed at 588 nm.

Adsorption Studies

Batch adsorption experiments were performed to evaluate the removal efficiency of Trypan Blue (TB) dye using the synthesized SA-g-poly(AAC-co-PVA) hydrogel. All experiments were conducted in 100 mL of dye solution using a water bath shaker at 120 rpm and 30°C. To investigate the effect of initial dye concentration, solutions at 50-500 mg L^{-1} were used with a fixed hydrogel dosage of 0.07 g. The effect of adsorbent dosage was studied by varying the hydrogel amount (0.01–0.10 g) in a dye solution with a constant concentration of 200 mg L^{-1}. The influence of solution pH was examined at values of 3, 7, 8, and 10 by adjusting the pH with 0.1 M HCl and 0.1 M NaOH solution. After reaching equilibrium, the residual dye concentration was determined using a UV-Vis spectrophotometer at (λ_{max}) of 588 nm. The equilibrium adsorption capacity (Q_e $mg.g^{-1)}$ and removal percentage (R%) were calculated using the following equations (3) and (4):

$$Q_e = \frac{(C_o - C_e)V}{W} \quad (3)$$

$$R_{\%} = \frac{C_0 - C_e}{C_0} 100 \quad (4)$$

where Q_e (mg. g^{-1}) denotes the equilibrium adsorption capacity; C_0 and C_e (mg. L^{-1}) represent the initial and equilibrium concentrations of Trypan Blue dye, respectively; V (L) refers to the solution volume of TB dye, and W (g) indicates the mass of the dry hydrogel.

Characterization Techniques

The surface functional groups of the synthesized SA-g-poly(AAC-co-PVA) hydrogel were identified using Fourier Transform Infrared Spectroscopy (FTIR) in the spectral range of 400–4000 cm^{-1}. The surface morphology and porous structure were examined using Field Emission Scanning Electron microscopy (FESEM). To investigate the internal structure and nanoscale particle-size distribution, Transmission Electron Microscopy (TEM) was used. The crystalline nature of the prepared hydrogel was analyzed by X-ray Diffraction (XRD) using Cu-Kα radiation. Furthermore, the thermal stability and degradation behavior of the hydrogel were evaluated using thermogravimetric analysis (TGA) over a temperature range of 25–600°C under a nitrogen atmosphere.

Adsorption Isotherm Models

Nonlinear isotherm adsorption models effectively characterize the interaction between the adsorbent and adsorbate. In this study, the Freundlich and Langmuir isotherm models are employed to examine adsorption. The Freundlich isotherm model is calculated using equation 5:

$$Q_e = K_f C_e^{1/n} \quad (5)$$

The Langmuir isotherm is primarily used to describe the adsorption of dyes from aqueous solutions. The Langmuir isotherm nonlinear model is calculated from equation 6:

$$Q_e = \frac{q_m K_L C_e}{1+K_L C_e} \quad (6)$$

where Qe: amount adsorbed per unit mass of adsorbent at equilibrium ($mg.g^{-1}$), ($mol.g^{-1}$), C_e: equilibrium concentration ($mg.L^{-1}$), ($mol.L^{-1}$), and K_f: capacity factor or Freundlich constant empirical ($L.mg^{-1}$).

1/n: Freundlich exponent, if the (n) value reaches unity, the adsorption is linear; if the n value is above unity, then the adsorption process is physical; if the "n" value is below unity, the adsorption process is chemical.

Langmuir constant empirical, which represents maximum adsorption efficiency ($mg.g^{-1}$), K_L: Langmuir constant (L/mg) or the equilibrium constant of the adsorption process [20].

3. Results and Discussion

Characterization of SA-g-poly (AAC-co-PVA) Hydrogel

FTIR analysis before and after adsorption

The Fourier transform infrared (FTIR) spectra of the SA-g-poly(AAC-co-PVA) hydrogel before and after Trypan Blue adsorption are illustrated in Figure 2. The spectrum of the pristine hydrogel displays a broad absorption band in the region of 3200–3500 cm^{-1}, which is attributed to the stretching vibrations of hydroxyl (–OH) groups associated with sodium alginate and poly(vinyl alcohol), indicating strong hydrogen bonding interactions within the polymeric network [21].

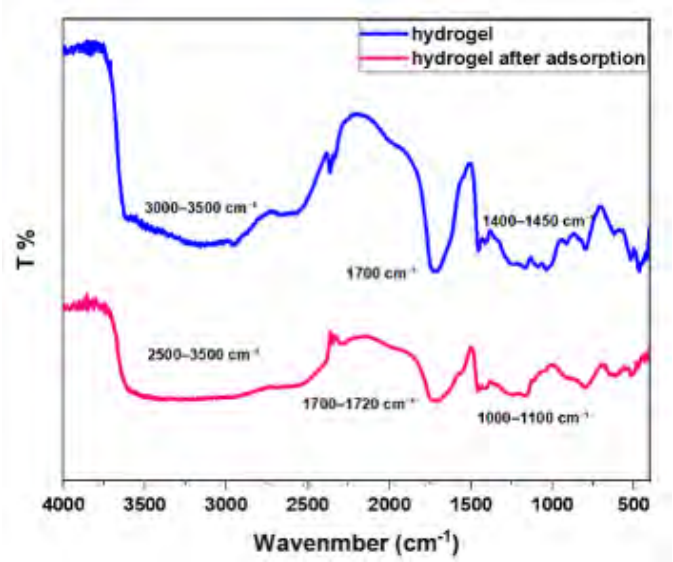

Fig 2. FTIR Spectra of the Synthesized Hydrogel Before and After Trypan Blue Adsorption

The absorption band observed around 1700–1720 cm^{-1} corresponds to the carbonyl (C=O) stretching vibration of acrylic-based units, confirming successful grafting and cross-linking of the polymer chains. In addition, the bands located near 1400–1450 cm^{-1} are assigned to the symmetric stretching vibrations of carboxylate ($–COO^-$) groups, while the peaks appearing in the range of 1000–1100 cm^{-1} are related to C–O and C–O–C stretching vibrations of the polysaccharide backbone [22,23].

After adsorption of Trypan Blue, noticeable changes in the FTIR spectrum were observed, including slight shifts and decreases in the intensity of the –OH and $–COO^-$ related bands. These variations indicate the involvement of hydroxyl and carboxyl functional groups in the adsorption process via electrostatic interactions and hydrogen bonding. The preservation of the prominent characteristic absorption bands after adsorption suggests that the hydrogel framework remains structurally stable during dye uptake [24,25].

Surface morphology analysis (FESEM)

The surface morphology of the prepared hydrogel before and after Trypan Blue adsorption was examined using field-emission scanning electron microscopy (FESEM), as shown in Figure 3a. The FESEM image of the pristine hydrogel reveals a highly porous, interconnected three-dimensional network with irregular cavities distributed throughout the surface. This porous structure is typical of alginate-based hydrogels prepared via free-radical graft polymerization and provides numerous accessible pathways that facilitate dye diffusion and adsorption processes [26,27].

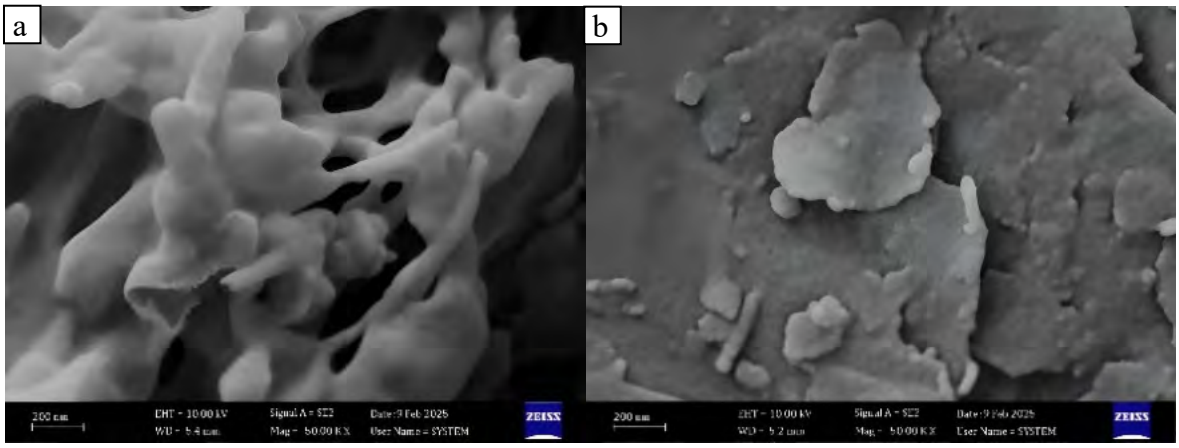

Fig 3. FESEM Images of SA-g-poly (AAC-co-PVA) Hydrogel (a) Before and (b) After the Adsorption Process

After adsorption (Figure 3b), the hydrogel surface becomes denser and partially covered by aggregated layers, indicating effective attachment of Trypan Blue molecules to the hydrogel matrix. The observed reduction in visible pore openings indicates that dye molecules occupy both internal pores and active surface sites via a combination of surface interactions and pore-filling mechanisms. Despite these morphological changes, the three-dimensional network framework remains largely preserved, demonstrating sufficient mechanical stability of the hydrogel during adsorption. This structural integrity is a key factor in maintaining regenerative capability and enabling repeated adsorption cycles [28,29].

Internal structure analysis (TEM)

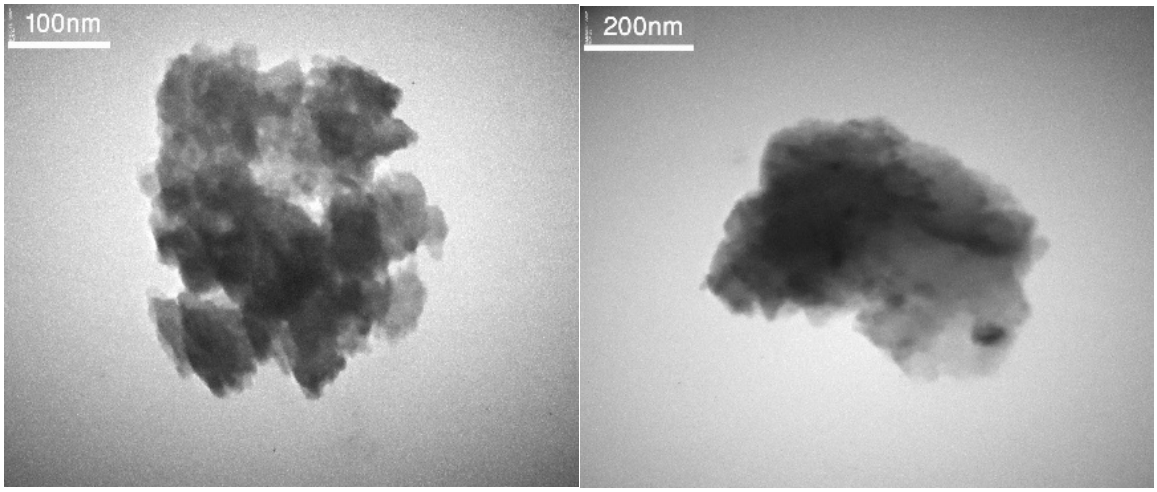

Fig 4. TEM Images of the Hydrogel's Internal Morphology at Different Magnifications

The internal morphology of the prepared hydrogel was investigated using transmission electron microscopy (TEM), as shown in Figure 4. The TEM images reveal irregular agglomerated regions containing nanoscale features dispersed throughout the polymeric matrix. These darker contrast areas correspond to polymer-rich domains formed during grafting and cross-linking and are commonly observed in biopolymer-based superabsorbent hydrogels [30].

At higher magnification, the hydrogel displays clustered internal domains with nonuniform boundaries and a relatively compact network. This structural appearance suggests that acrylic-based grafting onto the alginate backbone leads to the formation of dense nanoscale regions embedded within the swollen hydrogel network. Such features are beneficial for adsorption, as they facilitate dye diffusion and increase the number of accessible interaction sites. In addition, the absence of distinct crystalline lattice fringes confirms the predominantly amorphous nature of the hydrogel, which is advantageous for adsorption applications and is consistent with the XRD observations [31].

X-ray Diffraction (XRD) analysis

The X-ray Diffraction (XRD) pattern of the prepared SA-g-poly (AAC-co-PVA) hydrogel is presented in Figure 5. The diffractogram is characterized by a broad amorphous halo extending over the 2θ range of approximately 15–25°, while distinct crystalline peaks are absent.

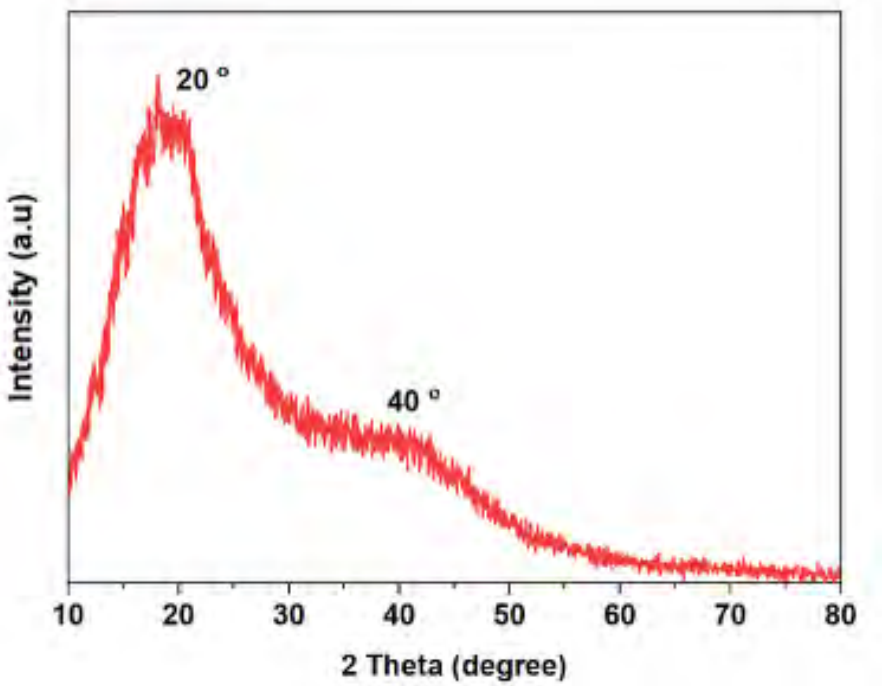

Fig 5. X-ray Diffraction (XRD) Pattern of the Prepared Hydrogel

This feature indicates that the synthesized hydrogel predominantly possesses an amorphous structure. Such diffraction characteristics are frequently reported for

polysaccharide-based hydrogels obtained via graft polymerization and cross-linking processes, in which the introduction of synthetic polymer chains interferes with the regular packing of the biopolymer backbone [32,33].

The suppression of crystalline features can be attributed to the grafting of acrylic segments onto alginate chains and to the physical entanglement of PVA within the three-dimensional cross-linked network. Such structural rearrangements hinder long-range crystalline order and result in a homogeneous amorphous matrix, as reported for alginate- and acrylic-based hydrogel nanocomposites.

The predominance of the amorphous structure is favorable for adsorption processes because it provides greater flexibility of the polymer chains and improves the exposure of functional groups, including hydroxyl (–OH) and carboxyl ($–COO^-$) moieties. Such structural characteristics facilitate more effective interactions between Trypan Blue molecules and the available active sites within the hydrogel network, thereby enhancing adsorption performance [34].

Thermal stability analysis (TGA)

The thermal stability of the prepared alginate–acrylic–PVA hydrogel was evaluated using thermogravimetric analysis (TGA), as illustrated in Figure 6. The resulting TGA profile shows a stepwise weight-loss pattern, which is commonly observed for cross-linked polysaccharide-based grafted hydrogels.

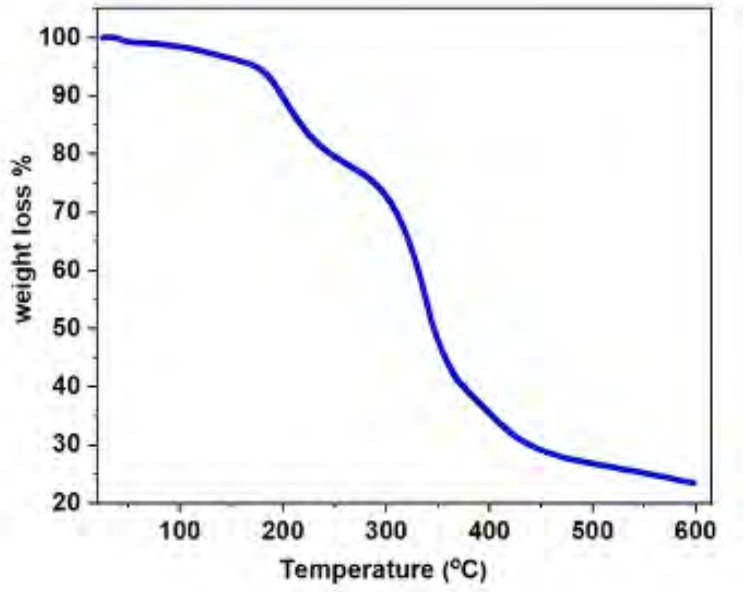

Fig 6. TGA Thermogram of the Alginate–Acrylic–PVA Hydrogel

An initial minor mass loss occurs below approximately 120°C and is mainly related to the release of physically adsorbed and weakly bound water molecules within the hydrogel structure. A second degradation stage is evident in the temperature range of 200–300°C and is attributed primarily to the thermal decomposition of grafted acrylic

components, as well as to the breakdown of pendant functional groups formed during grafting process [35,36]. At temperatures exceeding 300°C, a more substantial weight loss is observed, corresponding to the degradation of the alginate and PVA backbone chains and the progressive collapse of the three-dimensional cross-linked network. The overall degradation behavior, together with the presence of a measurable residual mass at higher temperatures, suggests that the incorporation of acrylic units and PVA chains contributes to improving the thermal stability of native alginate. This observation confirms the formation of a structurally stable, cross-linked hydrogel suitable for adsorption under a range of thermal conditions [37].

Optimization of Reaction Parameters

The synthesis conditions of the SA-g-poly(AAC-co-PVA) hydrogel were systematically optimized to maximize its swelling performance. The effects of reaction time and temperature were evaluated while keeping the concentrations of KPS (0.05 g), MBA (0.05 g), and acrylic acid (0.14 mol L^{-1}) constant.

Effect of reaction time

The reaction time was varied from 2 to 4 h at 60°C. As shown in Figure 7a, the hydrogel exhibited a maximum swelling ratio of 488% at 2 h. Shorter reaction times limit polymer chain growth and network formation, whereas longer reaction times increase crosslinking density by prolonging radical activity. This excessive crosslinking reduces network flexibility and pore size, restricting water penetration and leading to decreased swelling beyond the optimal time [38-40].

Effect of reaction temperature

The reaction temperature was varied from 55 to 75°C in 5°C increments (Figure 7b). Swelling increased with temperature, reaching a maximum of 530% at 75°C. The initial increase is attributed to enhanced thermal decomposition of the initiator (KPS), which generates more free radicals and promotes efficient grafting and network formation. This results in a more open and porous hydrogel structure that favors water uptake. However, at temperatures above the optimum, excessive radical activity increases crosslink density and can lead to chain termination, resulting in a more compact network and reduced swelling [41,42].

Effect of solvent volume

As shown in Figure 7c, the swelling percentage initially increases with increasing solvent volume, reaches a maximum at 100 mL, and then declines.

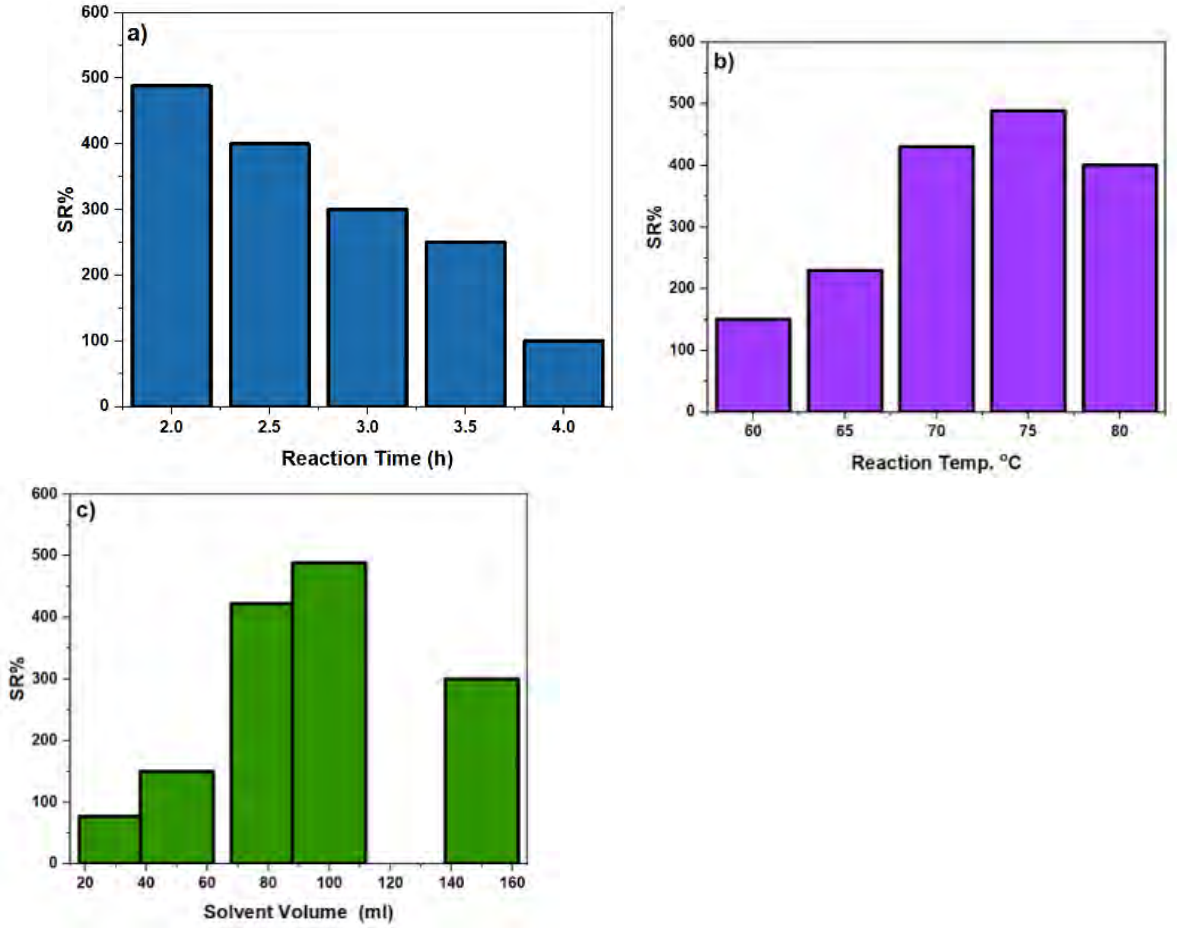

Fig 7. Effect of Several Parameters on the Highest Swelling Percentage of Hydrogel (a) Reaction Time, (b) Reaction Temperature, (c) Solvent Amount

The initial enhancement in swelling is attributed to improved dispersion of monomers and initiator in a larger solvent volume, which facilitates efficient free-radical generation and promotes uniform polymerization and network formation. This results in a more open and porous hydrogel structure that favors water uptake. However, beyond the optimal solvent volume, excessive dilution reduces the frequency of effective radical–monomer collisions, thereby lowering crosslinking efficiency and weakening network formation, thereby decreasing swelling capacity [43,44]. Overall, both reaction time and temperature strongly influence the balance between network formation and crosslinking density. Optimal swelling is achieved when the hydrogel network is sufficiently crosslinked to maintain structural integrity while remaining sufficiently flexible and porous to maximize water absorption [45,46].

Effect of Operational Parameters on Trypan Blue Adsorption

Effect of solution pH

The role of solution pH in controlling Trypan Blue adsorption onto the alginate–acrylic–PVA hydrogel was examined across a pH range of 3–11, as presented in Figure 8. A clear decrease in both removal efficiency (E%) and adsorption capacity (Q_e) was observed with increasing pH, At pH 3, the hydrogel showed high adsorption performance, with E = 96% and Q_e = 480 mg g^{-1} [47,48]. In contrast, at pH 11, both values decreased markedly to E = 41% and Q_e = 210 mg g^{-1}, demonstrating the pronounced decline in adsorption with increasing pH. indicating that acidic conditions favor dye uptake.

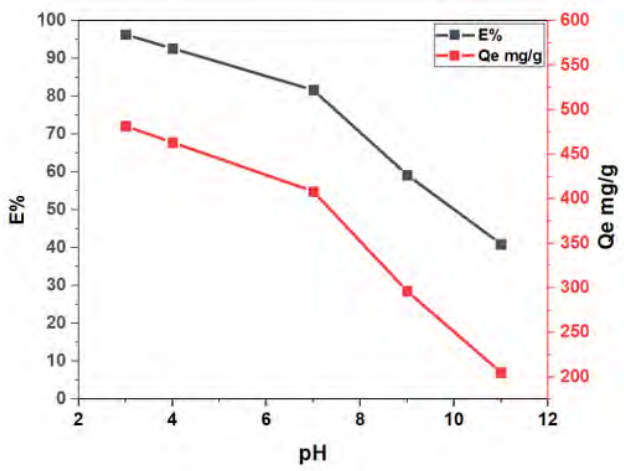

Fig 8. Effect of Solution pH on TB Dye Adsorption, Adsorption Conditions: 30°C, 200 mg L^{-1} Dye, 0.07g Hydrogel

This behavior is associated with changes in the surface charge of the hydrogel arising from the ionization state of functional groups within the alginate/PVA network, particularly carboxylic (–COOH/–COO^-) and hydroxyl (–OH) moieties. Under acidic conditions, protonation converts –COO^- groups into their neutral –COOH form, which lowers electrostatic repulsion between the hydrogel surface and the anionic sulfonate groups (–SO_3^-) of the dye. As a result, adsorption is enhanced through a combination of electrostatic attraction and hydrogen-bonding interactions. Similar pH-controlled adsorption behavior has been reported for polysaccharide- and acrylic-based hydrogel adsorbents. In contrast, under alkaline conditions, deprotonation increases the density of –COO^- sites, thereby strengthening electrostatic repulsion against anionic dye species and weakening adsorption, consistent with charge-governed adsorption observed for related hydrogel systems [49,50].

Point of zero charge (PZC)

Because the adsorption behavior of materials is strongly governed by their surface characteristics, determining the point of zero charge (PZC) provides essential insight into surface charge properties. In this study, the PZC of the (SA-g-poly(AAC-co-PVA)) hydrogel was determined using the pH drift method, a reliable technique for surface characterization. The PZC is the pH at which the net surface charge, including both internal and external sites, is zero. Below pHpzc, the hydrogel surface acquires a positive charge, whereas above pHpzc it becomes negatively charged.

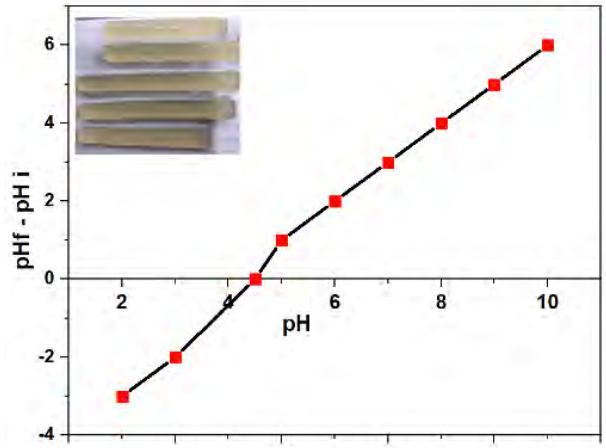

Fig 9. Effect of PZC of the (SA-g-poly(AAC-co-PVA)) Hydrogel

As illustrated in Figure 9, the initial pH (pHi) was plotted against the difference between the initial and final pH (ΔpH) after introducing a fixed amount of hydrogel into a 0.1 N NaCl solution. The pHpzc value was determined to be 4.5, indicating that under typical experimental conditions, the hydrogel surface predominantly carries a negative charge. This behavior suggests that the functional groups along the polymer chains play a key role in governing the surface charge and, consequently, the adsorption performance of the hydrogel [51,52].

Effect of adsorbent dosage

The effect of adsorbent dosage on Trypan Blue adsorption was examined by increasing the hydrogel mass from 0.01 to 0.10 g (Figure 10). As the dosage increased, the removal efficiency (E%) rose markedly, which is mainly attributed to the higher availability of adsorption sites and the larger effective surface area provided by increasing amounts of hydrogel in the solution. For example, increasing the hydrogel mass from 0.01 g to 0.10 g increased E% from ~50% to ~97% (Figure 10).

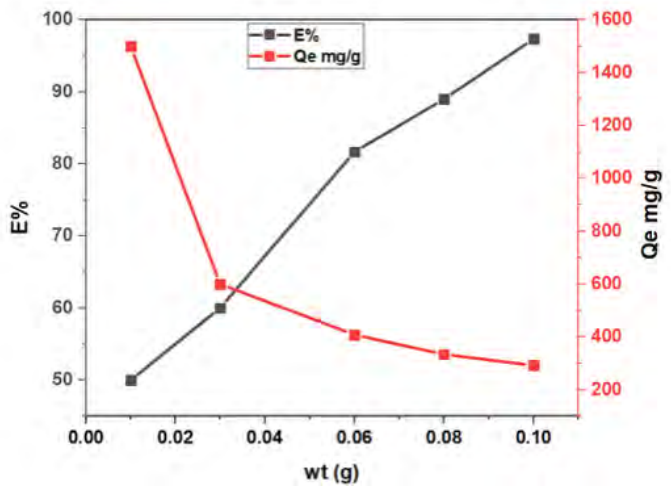

Fig 10. Effect of SA-g-poly(AAC-co-PVA) Hydrogel Dosage on Trypan Blue Adsorption, Adsorption Conditions: 30°C, 200 mg L^{-1} Dye , pH 7

In contrast, the adsorption capacity per unit mass (Qe, mg g^{-1}) decreased with increasing dosage. This behavior is commonly observed for hydrogel-based adsorbents when a fixed initial dye concentration is used, where many adsorption sites remain unsaturated at higher adsorbent dosages. Additionally, increasing hydrogel mass may lead to partial aggregation of swollen polymer domains, thereby reducing the accessibility of internal adsorption sites and decreasing Qe despite improved overall dye removal. Consistent with this, Q_e decreased from ~1500 mg g^{-1} at 0.01 g to ~300 mg g^{-1} at 0.10 g, confirming the opposite trends of E% and Qe with increasing hydrogel dosage [53,54].

Effect of initial Trypan Blue concentration

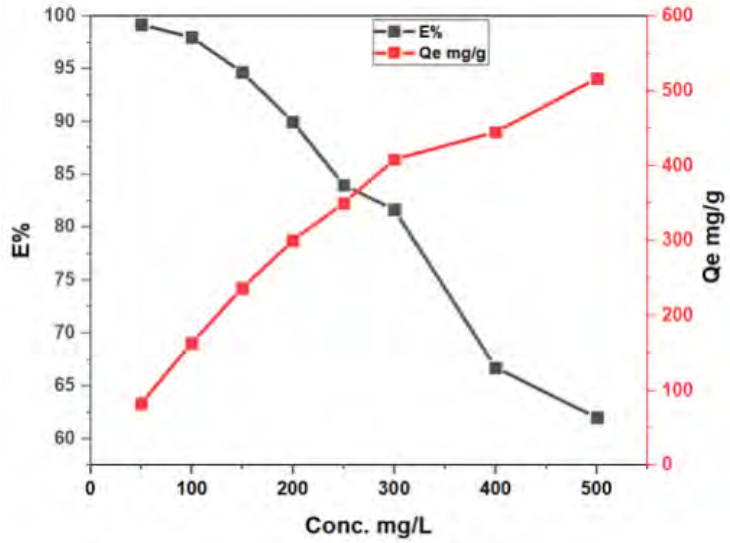

Fig 11. Effect of Initial Trypan Blue Concentration on Adsorption Behavior of the SA-g-poly(AAC-co-PVA) Hydrogel, Adsorption Conditions: 30°C, pH 7, 0.07g Hydrogel

The effect of the initial Trypan Blue concentration on the adsorption performance of the SA-g-poly(AAC-co-PVA) hydrogel was examined over a concentration range of 50–500 mg L^{-1}, as illustrated in Figure 11. An increase in dye concentration was accompanied by a gradual reduction in removal efficiency (E%), whereas the adsorption capacity (Q_e) showed a continuous increase. As shown in Figure 11, increasing the initial Trypan Blue concentration from 50 mg L^{-1} to 500 mg L^{-1} resulted in a noticeable decrease in E, from about 98% at 50 mg L^{-1} to nearly 62% at 500 mg L^{-1}, while Q_e increased significantly from approximately 90 mg g^{-1} to around 520 mg g^{-1} over the same concentration range. At lower concentrations, the abundance of available adsorption sites relative to the number of dye molecules promotes more efficient uptake, thereby increasing removal efficiency. With further increases in the initial concentration, these sites become progressively saturated, intensifying competition among dye molecules and resulting in a noticeable decline in E% [55].

In contrast, the continuous increase in Q_e at higher initial concentrations is attributed to the steeper concentration gradient between the bulk solution and the hydrogel surface, which enhances the mass-transfer driving force and allows greater dye accumulation per unit mass of adsorbent. The opposite trend between E% and Qe with increasing initial dye concentration is characteristic of hydrogel-based adsorbents and has been reported for polysaccharide–acrylic hydrogel systems used in dye adsorption studies [56,57].

Effect of contact time

The effect of contact time on Trypan Blue uptake by the SA-g-poly (AAC-co-PVA) hydrogel is presented in Figure 12. The adsorption capacity (Q_e) increases rapidly during the initial stage, reaching approximately 350 mg/g after about 25 min, which is attributed to the abundance of available active sites and the high concentration gradient between the solution and the hydrogel surface.

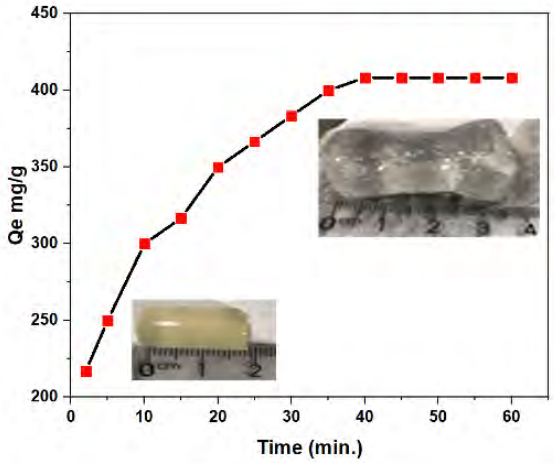

Fig 12. Effect of Contact Time on Trypan Blue Adsorption by the Prepared Hydrogel, Adsorption Conditions: 30°C, 200 mg L^{-1} Dye, 0.07g Hydrogel, pH 7

Beyond this period, the adsorption rate gradually decreases, and equilibrium is attained after approximately 40 min, with a maximum Qe of approximately 410 mg/g. This behavior is related to the progressive occupation of adsorption sites and the development of diffusion resistance within the cross-linked hydrogel network. Similar time-dependent adsorption profiles have been widely reported for polysaccharide-based hydrogels and bio-adsorbents used for dye removal [58].

Adsorption Isotherm

The equilibrium adsorption data of Trypan Blue onto the prepared hydrogel was evaluated using the Langmuir (monolayer) and Freundlich (multilayer) isotherm models, as shown in Figure 13.

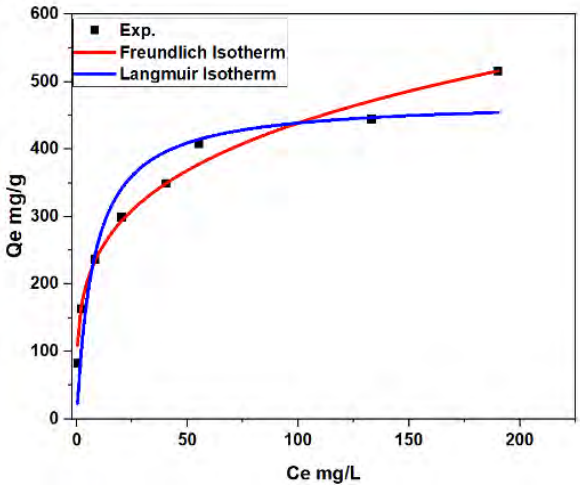

Fig 13. Equilibrium Adsorption Isotherms of TB Dye onto the Prepared Hydrogel, Showing Experimental Data and Fitting with Langmuir and Freundlich Models Under the Studied Conditions

At the same time, the corresponding fitting parameters are summarized in Table 1.

Table 1. Different Parameters of Isotherm Models for TB Dye Adsorption onto the Prepared Hydrogel

Isotherm model	Parameter	Value
Freundlich $Q_e = K_f C_e^{1/n}$	K_f	437.76 ± 10.05
	1/n	0.251 ± 0.017
	R^2	0.9838
Langmuir $Q_e = \frac{Q_m K_L C_e}{1 + K_L C_e}$	Q_m	493.09 ± 36.87 mg g^{-1}
	K_L	0.128 ± 0.050 L mg^{-1}
	R^2	0.8961

The fitting results indicated that the Freundlich model provides a superior description of the experimental data, as evidenced by its higher correlation coefficient (R^2 = 0.983) than the Langmuir model (R^2 = 0.896). This indicates that the adsorption process predominantly follows a multilayer mechanism on a heterogeneous hydrogel surface rather than uniform monolayer coverage [59].

The predominance of the Freundlich model suggests that Trypan Blue molecules interact with adsorption sites of different energies distributed within the grafted polymeric network of the hydrogel. Such adsorption behavior is commonly reported for alginate- and polysaccharide-based hydrogels and reflects the structural complexity and non-uniform surface characteristics inherent to these materials [60,61].

Regeneration Efficiency

The regeneration and reusability performance of the prepared hydrogels was evaluated over five consecutive adsorption–desorption cycles, as illustrated in Figure 14. The hydrogel exhibited an initial removal efficiency of approximately 82%, which gradually decreased with increasing regeneration cycles.

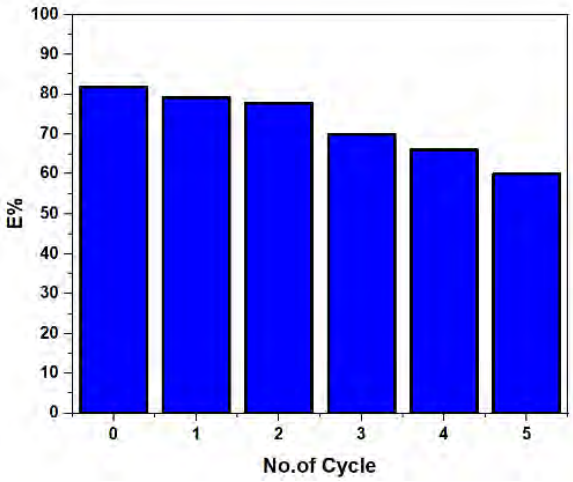

Fig 14. Effect of Regeneration Cycles on Adsorption Efficiency ($E_{\%}$)

After the second cycle, the removal efficiency changed little, remaining around 78%, indicating acceptable preservation of the hydrogel framework and accessibility of a considerable fraction of adsorption sites [62,63]. From the third cycle onward, a more pronounced decrease became evident, and the efficiency dropped to approximately 60% by the fifth cycle. This decline is likely attributable to cumulative effects arising from repeated use, including partial obstruction of active sites, incomplete release of adsorbed dye molecules during desorption, and minor structural fatigue within the crosslinked polymer network. Comparable regeneration trends have been reported for polysaccharide-based and grafted hydrogel systems, supporting the feasibility of employing such materials for multiple adsorption–desorption cycles [64,65].

Comparative Analysis with Existing Adsorbents

To evaluate the adsorption efficiency of the synthesized (SA-g-poly(AAC-co-PVA)) hydrogel for the removal of the anionic Trypan Blue (TB) dye from aqueous solutions, a comparative analysis was performed against previously reported adsorbents. Although direct comparisons are constrained by differences in experimental parameters, including operating conditions and adsorption environments, the results summarized in Table 2 indicate that the prepared hydrogel exhibits a notably high maximum adsorption capacity. These findings highlight the competitive performance and potential applicability of the synthesized hydrogel as an effective adsorbent for removing anionic and cationic dyes.

Table 2. Adsorption Capacity of (SA-g-poly(AAC-co-PVA)) Hydrogel for the Removal of Dyes

Sorbent/Hydrogel	Dye	Qe mg/g	Ref
St-g-AA(H)-AAM	MG	23.59	[66]
Hydrogel/Fe_3O_4	MB	9.76	[67]
BMEP-PVPA hydrogel	MB	284.4	[68]
Chitosan/Fe3O4	MB	9.65	[69]
Alginate/PP beads	ST	30.66	[70]
GG/bacterial cellulose	ST	17.57	[71]
XG-cl-poly (MEMA)/TiO_2	CV	160.33	[26]
Fly ash/TiO_2 - chitosan	MB	55.85	[72]
CMC-g-poly (AA-co-IA) /MMT	ST	19.024	[73]
SA-g-poly(AAC-co-PVA) hydrogel	TB	493.33	In this study

4. Conclusion

The present study demonstrates that a cross-linked SA-g-poly(AAC-co-PVA) hydrogel can effectively remove Trypan Blue (TB) from aqueous solutions. Spectroscopic and microscopic characterizations (FTIR, FESEM, TEM, and XRD) verified the successful formation of a porous and mainly amorphous hydrogel structure, which is advantageous for adsorption processes. The adsorption behavior was found to be highly dependent on the experimental conditions. Acidic media promoted dye uptake, and the highest performance was observed at pH 3, where the removal efficiency exceeded 93%, owing to protonation of surface functional groups and reduced electrostatic repulsion with anionic dye species. The adsorption process proceeded rapidly, reaching equilibrium after approximately 40 min, at which point a high Qe of 410mg/g was achieved, reflecting the fast occupation of readily accessible adsorption sites. Initial dye concentration also played a key role in controlling adsorption performance. The highest removal efficiency was observed at an initial concentration of 50 mg L^{-1} (E% ≈ 98%), whereas increasing the concentration resulted in a gradual decrease in efficiency due to saturation of active sites. Regarding adsorbent dosage, increasing the hydrogel mass improved dye removal, and an optimal dosage of 0.10 g was identified, corresponding to ~95% removal efficiency. Beyond this dosage, the improvement in efficiency became less pronounced due to partial site underutilization.

Isotherm analysis revealed that the adsorption data were better described by the Freundlich model (R^2 = 0.983), indicating a heterogeneous adsorption surface. Furthermore, the hydrogel retained nearly 60% of its initial removal efficiency after multiple regeneration cycles, confirming its reasonable stability and potential for repeated use.

5. References

1. Singh V, Pandit C, Roy A, Pandit S, Rai AK, Rani A, Ranjan N, Rustagi S, Malik S. Degradation of food dyes via biological methods: A state-of-the-art review. *Bioresour. Technol. Rep.*, 2024, 25, 101780.
2. Sherugar P, Padaki M, Naik NS, George SD, Murthy DHK. Biomass-derived versatile activated carbon removes both heavy metals and dye molecules from wastewater with near-unity efficiency: Mechanism and kinetics. *Chemosphere*, 2022, 287, 132085.
3. Sharma S, Sharma G, Kumar A, AlGarni TS, Naushad M, Alothman ZA, Stadler FJ. Adsorption of cationic dyes onto carrageenan and itaconic acid-based superabsorbent hydrogel: Synthesis, characterization and isotherm analysis. *J. Hazard. Mater.*, 2021, 421, 126729. https://doi.org/126710.121016/j.jhazmat.122021.126729
4. Subhan H, Alam S, Shah LA, Ali MW, Farooq M. Sodium alginate grafted poly(N-vinyl formamide-co-acrylic acid)-bentonite clay hybrid hydrogel for sorptive removal of methylene green from wastewater. *Colloids Surf., A*, 2021, 611, 125853. https://doi.org/125810.121016/j.colsurfa.122020.125853
5. Stanciu MC, Nichifor M. Adsorption of anionic dyes on a cationic amphiphilic dextran hydrogel: Equilibrium, kinetic, and thermodynamic studies. *Colloid Polym. Sci.*, 2019, 297(1), 45-57.
6. Shen Y, Li B, Zhang Z. Super-efficient removal and adsorption mechanism of anionic dyes from water by magnetic amino acid-functionalized diatomite/yttrium alginate hybrid beads as an eco-friendly composite. *Chemosphere*, 2023, 336, 139233. https://doi.org/139210.131016/j.chemosphere.132023.139233
7. Sringeri Ganesh P, Kadri Jagadish D, Badalamoole V. Development of gum tragacanth-based graft copolymer hydrogel for the adsorptive removal of dyes from wastewater. *Macromol. Chem. Phys.*, 2025, 226(22), e00225.
8. Sourbh T. Synthesis, characterization and adsorption studies of an acrylic acid-grafted sodium alginate-based TiO_2 hydrogel nanocomposite. *Adsorpt. Sci. Technol.*, 2018, 36(1-2), 458–477.
9. Singh J, Weber ME. Kinetics of one-dimensional gel swelling and collapse for large volume change. *Chem. Eng. Sci.*, 1996, 51(19), 4499-4508. https://doi.org/4410.1016/0009-2509(4496)00254-00250
10. Silva EC, Soares VR, Nörnberg AB, Fajardo AR. Recyclable 3D-printed composite hydrogel containing rice husk biochar for organic contaminants adsorption in tap water. *ACS Appl. Polym. Mater.*, 2023, 5(10), 8415-8429.
11. Sorze A, Valentini F, Dorigato A, Pegoretti A. Development of a xanthan gum based superabsorbent and water retaining composites for agricultural and forestry applications. *Molecules*, 2023, 28(4), 1952. https://doi.org/1910.3390/molecules28041952
12. Sizovs A, McLendon PM, Srinivasachari S, Reineke TM.

Carbohydrate polymers for nonviral nucleic acid delivery. *Top. Curr. Chem.*, 2010, 296, 131-190.
13. Aljeboree AM, Jasim KK, Sabah NA. High-capacity dye adsorption by low-cost combo hydrogel: Kinetic, thermodynamic, and regeneration study. *J. Inorg. Organomet. Polym. Mater.*, 2025, 35(10), 8350-8373.
14. Shirsath SR, Patil AP, Bhanvase BA, Sonawane SH. Ultrasonically prepared poly(acrylamide)-kaolin composite hydrogel for removal of crystal violet dye from wastewater. *J. Env. Chem. Eng.*, 2015, 3(2), 1152-1162: https://doi.org/1110.1016/j.jece.2015.1104.1016
15. Shi W-Y, Ding C, Yan J-L, Han X-Y, Lv Z-M, Lei W, Xia M-Z, Wang F-Y. Molecular dynamics simulation for interaction of PESA and acrylic copolymers with calcite crystal surfaces. *Desalination*, 2012, 291, 8-14.
16. Choudhary S, Sharma K, Kumar V, Sharma V. RSM-CCD directed modeling and optimization of a low-cost adsorbent based on sodium dodecyl sulfate for the selective removal of malachite green and methylene blue dyes: Kinetics, isotherm, and thermodynamics analysis. *Microchem. J.*, 2024, 205, 111158.
17. Chen X, Zhang G, Hou F, Zhu J. Highly effective removal of basic fuchsin dye using carboxymethyl konjac glucomannan grafted acrylic acid-acrylamide/montmorillonite composite hydrogel. *Int. J. Biol. Macromol.*, 2024, 277, 134163. https://doi.org/134110.131016/j.ijbiomac.132024.134163
18. Zheng M, Cai K, Chen M, Zhu Y, Zhang L, Zheng B. pH-responsive poly(gellan gum-co-acrylamide-co-acrylic acid) hydrogel: Synthesis, and its application for organic dye removal. *Int. J. Biol. Macromol.*, 2020, 153, 573-582.
19. Rizwan M, Naseem S, Gilani SR, Durrani AI. Optimization of swelling and mechanical behavior of *Acer platanoides* cellulose combo hydro-gel. *Kuwait J. Sci.*, 2024, 51(2), 100177. https://doi.org/100110.101016/j.kjs.102024.100177
20. Abu-Zurayk RA, Al Bakain RZ, Hamadneh I, Al-Dujaili AH. Adsorption of Pb (II), Cr (III) and Cr (VI) from aqueous solution by surfactant-modified diatomaceous earth: Equilibrium, kinetic and thermodynamic modeling studies. *Int. J. Miner. Process.*, 2015, 140, 79-87.
21. Thakur S, Chaudhary J, Thakur A, Gunduz O, Alsanie WF, Makatsoris C, Thakur VK. Highly efficient poly(acrylic acid-co-aniline) grafted itaconic acid hydrogel: Application in water retention and adsorption of rhodamine B dye for a sustainable environment. *Chemosphere*, 2022, 303, 134917.
22. Thamer, B.M., A. Aldalbahi, Hameed MMA, El-Newehy MH. *In situ* preparation of novel porous nano-composite hydrogel as effective adsorbent for the removal of cationic dyes from polluted water. *Polymers*, 2020, 12(12), 3002. https://doi.org/3010.3390/polym12123002
23. Aljeboree AM, Hussein UA-R, Alkaim AF, Abd S, Alsultany FH, Altimari US. pH-Responsive biopolymer/nano-clay hydrogel beads for dual dye removal: Adsorption kinetics, isotherms, and reusability.

Polym. Bull., 2025, 82(16), 11357-11393.
24. Tshikovhi A, Motaung TE. Chitosan and guar-gum-based polymeric nano-composites for the adsorption of contaminants in water: Insights into adsorption capacities, mechanisms, and applications. *Desalin. Water Treat.*, 2024, 320, 100708. https://doi.org/100710.101016/j.dwt.102024.100708
25. Thombare N, Mishra S, Siddiqui MZ, Jha U, Singh D, Mahajan GR. Design and development of guar gum based novel, superabsorbent and moisture retaining hydrogels for agricultural applications. *Carbohydr. Polym.*, 2018, 185, 169-178. https://doi.org/110.1016/j.carbpol.2018.1001.1018
26. Taktak FF, Özyaranlar E. Semi-interpenetrating network based on xanthan gum-cl-2-(N-morpholin-oethyl methacrylate)/titanium oxide for the single and binary removal of cationic dyes from water. *Int. J. Biol. Macromol.*, 2022, 221, 238-255. https://doi.org/210.1016/j.ijbiomac.2022.1008.1139
27. Taktak F, Gökçe S. Ultrasound-assisted synthesis of biodegradable graphene oxide-based hydrogel nanocomposites for highly efficient and cost-effective removal of methyl orange from aqueous media. *J. Water Process Eng.*, 2024, 58, 104837.
28. Thakur S, Arotiba OA. Synthesis, swelling and adsorption studies of a pH-responsive sodium alginate–poly(acrylic acid) superabsorbent hydrogel. *Polym. Bull.*, 2018, 75(10), 4587-4606.
29. Teweldebrihan MD, Dinka MO. Methyl red adsorption from aqueous solution using *Rumex abyssinicus*-derived biochar: Studies of kinetics and isotherm. *Water*, 2024, 16. DOI: 10.3390/w16162237
30. Tang Y, Li M, Mu C, Zhou J, Shi B. Ultrafast and efficient removal of anionic dyes from wastewater by polyethyleneimine-modified silica nanoparticles. *Chemosphere*, 2019, 229, 570-579.
31. Vahid B, Hossein P, Mohammad SA, Dariush S, Siamak J. Synthesis and characterization of bio-nano-composite hydrogel beads based on magnetic hydroxyapatite and chito-san: A pH-sensitive drug delivery system for potential implantable anticancer platform. *Polym. Bull.*, 2023, 23, 1223. https://doi.org/1210.1007/s00289-00023-05072-00281
32. Vasiraja N, Prabhahar RSS, Joshua A. Preparation and physio–chemical characterisation of activated carbon derived from *Prosopis juliflora* stem for the removal of methylene blue dye and heavy metal containing textile industry effluent. *J. Cleaner Prod.*, 2023, 397, 136579.
33. Varaprasad K, Jayaramudu T, Sadiku ER. Removal of dye by carboxymethyl cellulose, acrylamide and graphene oxide via a free radical polymerization process. *Carbohydr. Polym.*, 2017, 164, 186-194. https://doi.org/110.1016/j.carbpol.2017.1001.1094
34. Wahyu ME, Damayanti D, Wu HS. Production, characterization, and application of KOH-activated biochar from rice straw for azo dye adsorption. *Biomass*, 2025, 5, 40. DOI: 10.3390/biomass5030040
35. Wan S, Zhao W, Xiong D, Li S, Ye Y, Du L. Novel alginate immobilized TiO_2 reusable functional hydrogel beads with high photocatalytic

removal of dye pollutions. *J. Polym. Eng.*, 2022, 42(10), 978-985.
36. Wallenwein CM, Weigel V, Hofhaus G, Dhakal N, Schatton W, Gelperina S, Groeber-Becker FK, Dressman J, Wacker MG. Pharmaceutical development of nanostructured vesicular hydrogel formulations of rifampicin for wound healing. *Int. J. Mol. Sci*., 2022, 23(24).
37. Wan Z, Xiong Z, Ren H, Huang Y, Liu H, Xiong H, Wu Y, Han J. Graft copolymerization of methyl methacrylate onto bamboo cellulose under microwave irradiation. *Carbohydr. Polym.*, 2011, 83(1), 264-269.
38. Wei J, Yan L, Zhang Z, Hu B, Gui W, Cui Y. Carbon nanotube/chitosan hydrogel for adsorption of acid red 73 in aqueous and soil environments. *BMC Chem.*, 2023, 17(1), 104.
39. Wang Y, Shen Z, Wang H, Song Z, Yu D, Li G, Liu X, Liu W. Progress in research on metal ion crosslinking alginate-based gels. *Gels*, 2025, 11, 16. DOI: 10.3390/gels11010016
40. Aljeboree AM, Hussein SA, Altimari US, Mohealdeen SM, Alsultany FH, Alkaim AF. Optimization of swelling and mechanical behavior of novel pH-sensitive terpolymer biocomposite hydrogel based on activated carbon for removal brilliant blue dye from aqueous solution. *Polym. Bull.*, 2025, 82(5), 1447-1478. https://doi.org/1410.1007/s00289-00024-05588-00280
41. Winning D, Wychowaniec JK, Wu B, Heise A, Rodriguez BJ, Brougham DF. Thermoresponsiveness across the physiologically accessible range: Effect of surfactant, cross-linker, and initiator content on size, structure, and transition temperature of poly(N-isopropylmethacrylamide) microgels. *ACS Omega*, 2024, 9(34), 36185-36197.
42. Wang Z, Ning A, Xie P, Gao G, Xie L, Li X, Song A. Synthesis and swelling behaviors of carboxymethyl cellulose-based superabsorbent resin hybridized with graphene oxide. *Carbohydr. Polym.*, 2017, 157, 48-56.
43. Wang J, Sawut A, Wumaer M, Simayi R, Aikebaier M. Preparation of chitosan quaternary ammonium salt-sodium alginate/poly acrylic acid hydrogel and its application in flexible sensing. *J. Mech. Behav. Biomed. Mater.*, 2026, 173, 107231. https://doi.org/107210.101016/j.jmbbm.102025.107231
44. Wang G, Li G, Huan Y, Hao C, Chen W. Acrylic acid functionalized graphene oxide: High-efficient removal of cationic dyes from waste-water and exploration on adsorption mechanism. *Chemosphere*, 2020, 261, 127736.
45. Xinyou M, Lan W, Shiqing G, Yanyan D, Yunqing Z, Chuanyi W, Eric L. Synthesis of a three-dimensional network sodium alginate–poly(acrylic acid)/attapulgite hydrogel with good mechanic property and reusability for efficient adsorption of Cu^{2+} and Pb^{2+}. *Env. Chem. Lett.*, 2018, 16, 653–658.
46. Xiao C, Yang M. Controlled preparation of physical cross-linked starch-g-PVA hydrogel. *Carbohydr. Polym.*, 2006, 64(1), 37-40. https://doi.org/10.1016/j.carbpol.2005.1010.1020
47. Yaarub NA, Alshrefi SM, Rafea FAM, Ahmed T, Al-Mamoori MHK, Al-Nafiey AK, Al-Kaim AF. Optical and morphological characterizations of element oxides compound (Y_2O_3/SeO_2) nano-composite structures synthesized *via* chemistry of

laser ablation. *J. Global Pharma Technol.*, 2018, 10(3), 536-544.
48. Xisto MR, Damacena DHL, de Araújo FP, Alves D, Honorio LMC, Peña-Garcia R, Almeida L, de Oliveira JA, Furtini MB, Osajima JA. Biopolymer gellan-gum-based TiO_2: A green alternative photocatalyst approach for removal of pollutants. *Water*, 2024, 16(2), 315.
49. Yang J, Shojaei S, Shojaei S. Removal of drug and dye from aqueous solutions by graphene oxide: Adsorption studies and chemometrics methods. *npj Clean Water*, 2022, 5(1), 5.
50. Yamakawa T, Tatami J, Komeya K, Meguro T. Synthesis of AlN powder from $Al(OH)_3$ by reduction–nitridation in a mixture of NH_3–C_3H_8 gas. *J. Eur. Ceram. Soc.*, 2006, 26, 2413-2418.
51. Aljeboree AM, Alkaim AF, Alsultany FH, Issa SK. Highly reusable nano adsorbent based on clay-incorporated hydrogel nanocomposite for cationic dye adsorption. *J. Inorg. Organomet. Polym. Mater.*, 2024, 35(2), 1165-1186. https://doi.org/10.1007/s10904-10024-03344-10905
52. Parveen R, Tarannum Z, Ali S, Fatima S. Nanoclay based study on protein stability and aggregation and its implication in human health. *Int. J. Biol. Macromol.*, 2021, 166, 385-400. 310.1016/j.ijbiomac.2020.1010.1197
53. Yang Y, Song S, Zhao Z. Graphene oxide (GO)/polyacrylamide (PAM) composite hydrogels as efficient cationic dye adsorbents. *Colloids Surf., A*, 2017, 513, 315-324.
54. Yang X, Zhang X, Feng X, Xu B, Du C, Zhang E, Shan M, Zhang Y. Novel porous hydrogel beads based on amidoxime modified polymer of intrinsic microporosity for efficient cationic dye removal. *Microporous Mesoporous Mater.*, 2024, 377, 113218. https://doi.org/113210.111016/j.micromeso.112024.113218
55. Yang Z, Ni R, Yang Y, Qi J, Lin X, Zhang Y, Wang L, Wu Y, Li X, Lu H. Carboxymethyl cellulose-based supramolecular hydrogel with thermo-responsive gel-sol transition for temporary plugging of oil pipeline in hot work. *Carbohydr. Polym.*, 2024, 324, 121556. https://doi.org/121510.121016/j.carbpol.122023.121556
56. Alzayd AAM, Radia ND. Novel pH-sensitive of organic composite (kc-g-poly(AAc-co-AAm)/bentonite), synthesis and characterization candidate as a carrier for controlled release system *in vitro* to some drugs. *Carbon Lett.*, 2024, 34(1), 505-517. https://doi.org/510.1007/s42823-42023-00674-42821
57. An J-K, Wang W-B, Wang A-Q. Preparation and swelling properties of a pH-sensitive superabsorbent hydrogel based on psyllium gum. *Starch/Stärke*, 2010, 62(10), 501-507.
58. Aljeboree AM, Ghazi HH, Hussein SA, Jawad MA, Khuder SA, Alkaim AF. Facile fabrication of a low-cost carboxymethyl cellulose–polyacrylamide composite for the highly efficient removal of cationic dye: Optimization, kinetic and reusability. *J. Iran. Chem. Soc.*, 2025, 22(1), 91-111. https://doi.org/110.1007/s13738-13024-03132-13735
59. Vadivelan V, Kumar KV. Equilibrium, kinetics, mechanism, and process design for the sorption of methylene blue onto rice husk. *J. Colloid Interface Sci.*, 2005, 286(1), 90-100.

60. Weber WJJ, Morris JC. Kinetics of adsorption on carbon from solution. *J. Sanit. Eng. Div., Am. Soc. Civ. Eng.*, 1963, 89, 31-59.
61. Wang ZK, Li T-T, Peng HK, Ren H, Lin JH, Lou C-W. Natural-clay-reinforced hydrogel adsorbent: Rapid adsorption of heavy-metal ions and dyes from textile wastewater. *Water Env. Res.*, 2022, 94.
62. Thamer BM, Shaker AA, Abdul Hameed MM, Al-Enizi AM. Highly selective and reusable nanoadsorbent based on expansive clay-incorporated polymeric nanofibers for cationic dye adsorption in single and binary systems. *J. Water Process Eng.*, 2023, 54, 103918. https://doi.org/103910.101016/j.jwpe.102023.103918
63. Aljeboree AM, Alkaim AF, Hussein SA, Alsultany FH, Jawad MA. Ecofriendly k-carrageenan-based hydrogel with strong adsorption and higher abilities to remove crystal violet from aqueous solution: Thermodynamic, isotherm and kinetic investigation. *J. Inorg. Organomet. Polym. Mater.*, 2025, 35(4), 2921-2942.
64. Usmanova GS, Latypova LR, Yusupova AR, Mustafin AG. Preparation of copolymers based on aniline and 2[2-chloro-1-methylbut-2-en-1-yl]aniline and their application for the removal of methyl orange from aqueous solutions. *J. Polym. Env.*, 2025, 33(3), 1585-1600. https://doi.org/1510.1007/s10924-10024-03419-x
65. Ullah N, Ali Z, Khan AS, Adalat B, Nasrullah A, Khan SB. Preparation and dye adsorption properties of activated carbon/clay/sodium alginate composite hydrogel membranes. *RSC Adv.*, 2024, 14(1), 211-221.
66. Al-Aidy H, Amdeha E. Green adsorbents based on polyacrylic acid-acrylamide grafted starch hydrogels: The new approach for enhanced adsorption of malachite green dye from aqueous solution. *Int. J. Env. Anal. Chem.*, 2021, 101(15), 2796-2816. https://doi.org/2710.1080/03067319.03062020.01711896
67. Rana VS, Sharma N. Adsorption profile of anionic and cationic dyes through Fe_3O_4 embedded oxidized Sterculia gum/gelatin hybrid gel matrix. *Int. J. Biol. Macromol.*, 2023, 232, 123098. https://doi.org/123010.121016/j.ijbiomac.122022.123012.123317
68. Anil I, Gunday ST, Bozkurt A, Alagha O. Design of crosslinked hydrogels comprising poly(vinylphosphonic acid) and bis[2-(methacryloy-loxy)ethyl] phosphate as an efficient adsorbent for wastewater dye removal. *Nanomaterials*, 2024, 10(1), 131. https://doi.org/110.3390/nano10010131
69. Zeng L, Xie M, Zhang Q, Kang Y, Guo X, Xiao H, Peng Y, Luo J. Chitosan/organic rectorite composite for the magnetic uptake of methylene blue and methyl orange. *Carbohydr. Polym.*, 2015, 123, 89-98. https://doi.org/10.1016/j.carbpol.2015.1001.1021
70. Abbaz A, Arris S, Viscusi G, Ayat A, Aissaoui H, Boumezough Y. Adsorption of safranin-O dye by alginate/pomegranate peels beads: Kinetic, isotherm and thermodynamic studies. *Gels*, 2023, 9(11), 961. https://doi.org/910.3390/gels9110916
71. Nguyen HT, Ngwabebhoh FA, Saha N, Saha T, Saha P. Gellan gum/bacterial cellulose hydrogel

crosslinked with citric acid as an eco-friendly green adsorbent for safranin and crystal violet dye removal. *Int. J. Biol. Macromol.*, 2022, 222, 77-89. https://doi.org/10.1016/j.ijbiomac.2022.1009.1040

72. Gajera R, Patel RV, Yadav A, Labhasetwar PK. Adsorption of cationic and anionic dyes on photocatalytic fly ash/TiO_2 modified chitosan biopolymer composite. *J. Water Process Eng.*, 2022, 49, 102993. https://doi.org/102910.101016/j.jwpe.102022.102993

73. Mohammadzadeh Pakdel P, Peighambardoust SJ, Arsalani N, Aghdasinia H. Safranin-O cationic dye removal from wastewater using carboxymethyl cellulose-grafted-poly(acrylic acid-co-itaconic acid) nanocomposite hydrogel. *Env. Res.*, 2022, 212, 113201. https://doi.org/113210.111016/j.envres.112022.113201